

Imaging Factors Impacting on Accuracy and Radiation Dose in 3D Printing

Jorge Javier de Lima Moreno¹ · Gabriela Salatino Liedke² · Roberto Soler¹ · Heloisa Emília Dias da Silveira³ · Heraldo Luis Dias da Silveira³

Received: 7 September 2016 / Accepted: 22 February 2018 / Published online: 28 February 2018
© The Association of Oral and Maxillofacial Surgeons of India 2018

Abstract

Objectives To compare reconstructed area and surface roughness of 3D models acquired using nine image acquisition protocols. Radiation dose was also compared among acquisition protocols.

Methods A dry craniofacial specimen was scanned using three CT devices (a cone beam CT, a 16-channel fan beam CT, and a 64-channel fan beam CT), with three different acquisition protocols each. Nine 3D models were manufactured using polylactic acid. Surface roughness and reconstructed area were determined for each 3D model. The radiation dose during acquisitions was measured using lithium crystals. ANOVA was used to compare the data among the 3D models. Linear function optimization techniques based on stochastic variables were applied to identify the most suitable protocol for use.

Results For surface roughness, statistically significant differences were observed among all 3D models and the specimen. For reconstructed area, CBCT and one CT-16 channel protocols originated 3D models statistically significant different from the specimen. Higher radiation doses were observed with fan beam CT acquisitions.

Conclusions All three CT devices were suitable for 3D printing when used at full resolution. The highest reconstruct

area vs. radiation dose ratio was found for 64-channel CT devices.

Keywords Multidetector computed tomography · Cone beam computed tomography · Radiation dosage · 3D printing

Introduction

Rapid prototyping of 3D models has enabled significant advances in cost-affordable diagnostic, planning and manufacturing technology for prosthesis applications. The use of biomodels has also increased the predictability of surgical procedures, leading to surgical time reduction, and to post-surgery conditions improvement [1]. Erickson et al. [2] reported that 69% of medical and dental specialists have used stereolithographic models for diagnostic purposes, and 73% for explanatory purposes—77% of the sample reported a reduction in surgical time.

Even though high success rates are associated with the use of rapid prototyping [3, 4], 3D models have been reported to differ from relevant anatomical structures in some studies. A biomodel should have some characteristics to enable its use, and to increase the rates of success, such as to include all of the anatomy of interest, to be free from any artefacts that result in deviating from the reality, and to have a smooth surface [5, 6]. Manufacturing methods, acquisition protocols, and patient's characteristics may cause errors on the 3D model, which could influence on preoperative planning or on surgical simulation [5, 7–9].

Developments of medical imaging applications and computer software enabled the easy manipulation of images obtained by computed tomography (CT) [10]. Whenever a CT examination is needed, it is important to have in mind the

✉ Jorge Javier de Lima Moreno
jjdelima76@gmail.com

¹ Department of Maxillofacial Prosthesis, School of Dentistry, Universidad de la Republica, Las Heras 1925, Montevideo, Uruguay

² Department of Stomatology, School of Dentistry, Federal University of Santa Maria, Santa Maria, Brazil

³ Department of Surgery and Orthopedics, School of Dentistry, Federal University of Rio Grande do Sul, Porto Alegre, Brazil

recommended principles of justification, optimization, and limitation of dose. Thus, an appropriate acquisition protocol should be selected, based on the selection of correct exposure parameters, field of view (FOV), and voxel size, depending on diagnostic needs [11–13]. The precision of rapid prototyping techniques also depends on a number of factors, such as scanner type (cone beam or fan beam), acquisition time, FOV, voxel size, slice thickness, pitch, gantry type, and image filters [14–16]. Despite several common features shared by cone beam CT (CBCT) and fan beam CT (FBCT) [17], CBCT can be conveniently used in dental applications in view of isotropic voxels, rapid scanning, easy availability, and low operating cost, in addition to low patient radiation dose [18, 19].

The aim of this study was to perform a throughout evaluation on the accuracy of 3D models manufactured based on different image acquisition protocols, comparing surface roughness, and reconstructed area. The radiation dose from the acquisition protocols was also compared.

Materials and Methods

Study Design

A cross-sectional observational in vitro study was conducted following approval by the Research & Ethics Committee of the Faculty of Dentistry (No. 22201). Nine 3D models were printed from a dry craniofacial specimen bounded by a line crossing the frontozygomatic sutures at the top, a line passing through the rear of pterygoid apophysis at the back, the occlusal plane with its palate vaulting at the bottom, and the anterior wall of the maxillary sinus, up to the alveolar ridge, at the front. The specimen used in this study was made available by the Museum of Anatomy of the Faculty of Dentistry.

Setting

Three CT devices were used for the acquisition of tomographic images: a CBCT (i-CAT tomography, Imaging Sciences International, Inc, Hatfield, PA, USA), a FBCT 16-channel (Bright Speed, General Electric, Milwaukee, Wisconsin, USA), and a FBCT 64-channel (SOMATOM Sensation, Siemens AG Medical Solutions, Erlangen, Germany). Image acquisition protocols for each of the CT devices are shown in Table 1. Two lithium crystal dosimeters (SAPRA, São Paulo, SP, Brazil) were attached to the anterior maxillary sinus wall in each of the CT acquisitions for radiation dose measurement. The specimen was immersed in a plastic vessel containing water in order to simulate soft tissue during acquisitions.

Data were exported in DICOM format and converted to .stl format using InVesalius 3 Beta 2 (CenPRA, Renato

Archer Research Center, Campinas, SP, Brazil). The same printer (PA2200; Sinterstation HiQ, 3D Systems Company, Valencia, CA, USA) was used to manufacture all 3D models, using selective laser sintering (SLS) technique in polylactic acid (PLA).

Data Collection

All nine 3D models and the specimen were tested for reconstructed area and surface roughness. Reconstructed area was determined by the filling material and calculated on photographs of the orbit floor. The 3D models and the specimen were placed in a standardized position, with the orbit floor facing up. The camera was fixed to a tripod (40 cm focus—object distance) with the focus perpendicular with the orbit floor surface. The photographs were imported into Image J software (National Institutes of Health, Bethesda, Maryland, USA). After image calibration, the orbit floor area (mm²) was delimited by a line starting at the inner orbital angle, running along the anterior edge of the pterygomaxillary fissure up to the infraorbital crest, and then medially, surrounding the tear duct, before returning to the inner corner of the eye orbit along the etmoidmaxillary suture (Fig. 1). The non-reconstructed area of the 3D models was also measured and subtracted from the studied area, and then the reconstructed area was obtained (%). The measurements from the right and the left sides were taken, and the mean value was used. All measurements were repeated after 15 days to ensure intra-examiner reproducibility (ICC > 0.9).

The surface roughness was determined by a roughness meter (Mitutoyo American Corporation SJ-201, Aurora, IL, USA) in units of roughness average (Ra). The external surface of the zygomatic bone was analyzed, and five readings per sample were recorded (Fig. 2).

The mean radiation dose from the two lithium crystal dosimeters was recorded for each of the nine exposure parameters.

Statistical Analysis

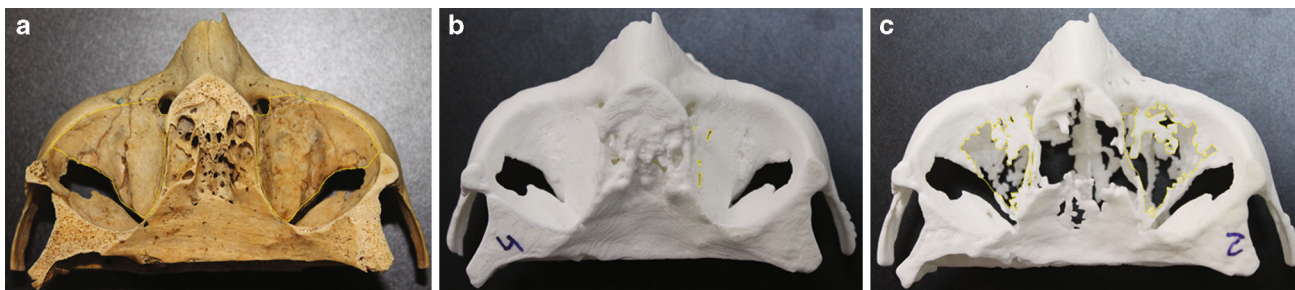
Surface roughness, reconstructed area, and radiation dose were compared using ANOVA, followed by post hoc Tukey test and Dunnett T3 for radiation dose. The level of statistical significance was $p < 0.05$.

Since the studied variables are expressed in different units of measurement, a linear function index was used to compare them. A linear optimization technique based on stochastic variables was applied using Risk Optimizer software (Palisade Corporation, Ithaca, NY, USA) to identify which protocol had the highest performance. The procedure was based on the linear function index, where $\times 1$ is the roughness (Ra), $\times 2$ is the reconstructed area (%),

Table 1 Acquisition protocols and CT devices for each 3D model coding scheme

Resolution (mm)	CB			CT-16			CT-64		
	0.2	0.25	0.3	0.625	1.25	2.5	0.75	1.0	1.5
kVp	120	120	120	120	120	120	120	120	120
mAs	30.89	30.89	15.44	100	100	100	90	90	90
FOV (mm)	8.5×	8.5×	8.5×	140	140	140	140	140	140
Exposure time (s)	140	140	140	5.2	5.2	5.2	3.12	3.12	3.12
Rot time (s)	23	23	8.5	0.8	0.8	0.8	0.5	0.5	0.5
Slice thickness				0.625	1.25	2.5	0.755	1.0	1.5
Pitch				0.62	0.6	1.25	0.4	0.5	0.7

CB cone beam computed tomography, CT-16 fan beam computed tomography 16-channel, CT-64 fan beam computed tomography 64-channel

**Fig. 1** a The bone specimen used presenting the evaluated reconstructed area; and two 3D models: b greatest reconstructed area CT-16 0.625 mm, and c smallest reconstructed area CB 0.3 voxel**Fig. 2** a The roughness meter used showing how the surface roughness was measured; and two 3D models: b greatest surface smoothness CT 64 1.25, and c greatest surface roughness CB 0.25 voxel

and $\times 3$ is the radioactive dose (mSv). Because the variables are positive, to maximize the above index, the second variable should be maximized while the first one and the third one should be minimized.

Results

Table 2 shows the comparisons for reconstructed area, surface roughness and radiation dose. All models achieved satisfactory reconstructed area: CT-16 0.625 reached the highest value (99.88% of the study area reconstructed), whereas CB 0.3 demonstrated the lowest reconstructed area (58.93%) (Fig. 1).

The results for surface roughness indicated statistically significant differences among all the 3D models and the specimen (Table 2). The protocol which differed the most from the specimen was the CB 0.25 (Fig. 2).

For radiation dose (Table 2), CBCT protocols showed lower values than FBCT devices. Voxel size was inversely related to radiation dose for CBCT protocols: the lower the voxel size, the higher the radiation dose. For FBCT devices, there was a direct relationship between these variables: the lower the voxel size, the lower the radiation dose, for both 16- or 64-channels CT.

To compare the variables shown in Table 2, results were normalized to zero and a standard deviation (SD) equal to

Table 2 Reconstructed area (%), raw roughness (Ra), and radiation dose (mSv) values for the bone specimen and each 3D model

	Reconstructed area	Roughness	Radiation dose
Specimen	100.000 ^A	2.288 ^A	
CB 0.2	89.042 ^B	7.870 ^{BCD}	2.450 ^A
CB 0.25	89.797 ^B	8.470 ^D	2.380 ^A
CB 0.3	58.930 ^C	7.160 ^{BCD}	1.230 ^B
CT-16 0.625	99.880 ^A	7.300 ^{BCD}	9.900 ^{DE}
CT-16 1.25	98.172 ^A	6.330 ^B	9.680 ^{CDE}
CT-16 2.5	85.953 ^B	6.970 ^{BCD}	11.600 ^E
CT-64 0.75	97.623 ^A	7.140 ^{BCD}	6.410 ^{CD}
CT-64 1.0	98.875 ^A	6.610 ^{BC}	8.065 ^{CD}
CT-64 1.5	96.032 ^A	8.130 ^{CD}	7.980 ^{CD}

CB cone beam computed tomography, CT-16 fan beam computed tomography 16-channel, CT-64 fan beam computed tomography 64-channel. CT devices are followed by voxel size. Numbers followed by upper case letters indicate comparisons among the 3D models. Different letters indicate the statistical difference at $p < 0.05$; ANOVA followed by Tukey’s multiple comparison test

1. The mean and the SD of each variable were calculated, and the following transformation was made: $Z_i = (x_i - \mu_i) / \sigma_i$, where μ_i is the mean value of variable i and σ_i is its SD. Results are shown in Table 3.

In order to discriminate the most suitable protocol, weight coefficients were applied to each studied variable (surface roughness—reconstructed area—radiation dose). Five different compositions (A, B, C, D and E) were proposed. In column A, the same coefficient was applied to the three variables, showing that CT-64 1.0 mm lead to the most accurate results. If reconstructed area and radiation dose are assigned higher weights (column B and C), CT-64 0.75 mm CT-64 1.0 mm appear as the best fit protocols. CB 0.2 voxel appears as the best option assuming that

Table 3 Normalized reconstructed area (%), roughness (Ra), and radiation dose (mSv) data for each 3D model

	Reconstructed area	Roughness Ra	Radiation dose
CB 0.2	0.767	– 0.112	– 1.111
CB 0.25	1.622	– 0.053	– 1.130
CB 0.3	– 0.244	– 2.458	– 1.436
CT-16 0.625	– 0.044	0.732	0.868
CT-16 1.25	– 1.426	0.599	0.810
CT-16 2.5	– 0.514	– 0.353	1.320
CT-64 0.75	– 0.272	0.557	– 0.059
CT-64 1.0	– 1.027	0.654	0.381
CT-64 1.5	1.138	0.433	0.358

CB cone beam computed tomography, CT-16 fan beam computed tomography 16-channel, CT-64 fan beam computed tomography 64-channel. CT devices are followed by voxel size

radiation dose has a higher weight than that the other variables (column D). If reconstructed area is assigned the highest weight coefficient (column E), the highest precision is associated with CT-16 0.625 mm, which reproduced 99.88% of the reconstructed area.

Applying linear optimization techniques and random variables with Risk Optimizer software, weight coefficients were selected randomly by Monte Carlo simulation and optimal values were determined. The software selected a 64-channel protocol 95% of the time, CT-64 1.0 mm or CT-64 0.75 mm over 85% of the time, with a marked preponderance of CT-64 0.75 mm (Table4).

Discussion

Rapid prototyping of 3D models is routinely used for diagnosis, communication and pre-surgical planning, but also for more complex procedures, such as the design and manufacture of implants and prosthesis [1–4]. Therefore, it is very advisable for those models be accurate. Despite the precision of CT-based 3D printing techniques, some studies have reported errors on reproducibility of anatomical details and on measurements, amounting to as much as 0.6 mm [11, 13, 20, 21], depending on the slice thickness of acquisition protocols and on the manufacturing method. This study evaluated the reconstructed area by comparing the bone tissue present on the specimen and on the 3D models. It was observed that a 16-channel CT device can be used conveniently at a 0.625 mm slice thickness to reconstruct 99.88% of the bone specimen. The reconstructed area of 3D models based on 64-channel FBCT acquisitions was as high as 98.8%, while CBCT protocols had the lowest values. Those results are in accordance with the literature, suggesting that 3D models based on FBCT can successfully reconstruct relevant anatomical structures [1, 3, 4].

The surface roughness of a 3D model is related to the layer thickness at which the model is built, and to the slice thickness of the CT acquisition protocol [8]. This study was based on the same manufacturing method (SLS), and therefore the results from surface roughness may be attributed to the differences on the acquisition protocols. Even though statistically significant differences were found among the specimen and the 3D models, the differences among the protocols were not great enough. Clinical implications of those differences should be further investigated.

The radiation dose is a constant concern among health professionals, and FBCT is associated with higher radiation exposure than CBCT [22]. In this study, those 3D models based on 16-channel CT showed the highest radiation dose, which was 1.39-fold higher than that found for 64-channel

Table 4 Weighted reconstructed area, roughness, and radiation dose data (numbers in brackets represent the variables' diverse weight coefficients for *surface roughness*; *reconstructed area*; *radiation dose*)

	A (1/3;1/3;1/3)	B (0.2;0.4;0.4)	C (0.2;0.35;0.45)	D (0.2.0.3.0.5)	E (0.03.0.92.0.03)
CB 0.2	0.08	0.25	0.31	0.37	− 0.09
CB 0.25	− 0.18	0.11	0.17	0.22	− 0.06
CB 0.3	− 0.26	− 0.36	− 0.17	0.03	− 2.26
CT-16 0.625	− 0.03	− 0.05	− 0.13	− 0.21	0.66
CT-16 1.25	0.41	0.20	0.13	0.06	0.58
CT-16 2.5	− 0.39	− 0.57	− 0.61	− 0.66	− 0.36
CT-64 0.75	0.30	0.30	0.28	0.25	0.53
CT-64 1.0	0.43	0.31	0.26	0.21	0.63
CT-64 1.5	− 0.35	− 0.20	− 0.24	− 0.28	0.36

CB cone beam computed tomography, CT-16 fan beam computed tomography 16-channel, CT-64 fan beam computed tomography 64-channel. CT devices are followed by voxel size

CT protocols. On the other hand, CBCT protocols provided a radiation dose 3.70-fold lower than that of 64-channel FBCT and 5.14-fold lower than that of 16-channel FBCT protocols.

Differences in radiation dose have been reported to depend directly on the mAs specified for each protocol [23]. In this research, protocols of 90 mAs for the 64-channel CT and 100 mAs for the 16-channel CT were used. The above explains the identification of three well-defined groups: CBCT, 64-channel FBCT and 16-channel FBCT protocols. It also explains the differences found among the CBCT protocols, as the mAs differed according to the protocol.

Various studies have addressed the suitability of CBCT for diagnostic and surgical planning applications in dentistry [18, 19]. Erickson et al. [2] reported that 70% of the 3D model requests are made by practitioners who want to study and plan clinical cases of high surgical complexity. The results of the present study indicate the use of CBCT at a 0.2 mm voxel, as it was the protocol with the greatest reconstructed area (89%), minimizing the radiation dose where explanatory purposes are sought.

Furthermore, if the clinical purpose of the 3D model is to manufacture oral maxillofacial prostheses, then the protocol leading to the greatest reconstructed area should be recommended in order to ensure the adjustment of the manufactured pieces [3–7]. In this study, the 3D models that led to the smoothest surface and to the highest reconstructed area were acquired with a 64-channel CT. The use of the 64-channel CT 0.75 mm protocol is recommended as it had lower radiation dose than the 64-channel CT 1.0 mm protocol. Therefore, for planning and explanatory purposes, CBCT scans at 0.2 voxel size are recommended, whereas for manufacturing of oral maxillofacial prostheses 64-channel FBCT at 0.75 mm voxel size seems to have better results.

Patient motion and presence of metal materials are among the sources of noise in CT acquisition, which could impair the manufacturing of biomodels [6, 24, 25]. Therefore, the present study was based on an in vitro model, without any metal structure, so the evaluation was restricted to the type of CT, and to the acquisition protocols. Furthermore, the specimen was immersed in water in order to simulate soft tissue, for x-ray attenuation before it reaches the bone.

Based on the results from the present study, it is possible to conclude that all CT devices proved to be suitable for 3D printing when used at full-resolution. Nevertheless, there were important differences concerning the reconstructed area of the 3D models and the radiation dose, which should guide the selection of the most appropriate acquisition protocol, correlating the indication purpose with the As Low As Reasonably Achievable (ALARA) principle.

Compliance with Ethical Standards

Conflict of interest The authors declare that they have no conflict of interest.

Ethical Approval This article does not contain any studies with human participants or animals performed by any of the authors.

References

1. Sannomiya EK, Silva JV, Brito AA, Saez DM, Angelieri F, Dalben Gda S (2008) Surgical planning for resection of an ameloblastoma and reconstruction of the mandible using a selective laser sintering 3D biomodel. *Oral Surg Oral Med Oral Pathol Oral Radiol Endod* 106:36–40
2. Erickson DM, Chance D, Schmitt S, Mathis J (1999) An opinion survey of reported benefits from the use of stereolithographic models. *J Oral Maxillofac Surg* 57:1040–1043
3. Sykes LM, Parrott AM, Owen CP, Snaddon DR (2004) Applications of rapid prototyping technology in maxillofacial prosthetics. *Int J Prosthodont* 17:454–459

4. Suomalainen A, Stoor P, Mesimäki K, Kontio RK (2015) Rapid prototyping modelling in oral and maxillofacial surgery: a two year retrospective study. *J Clin Exp Dent* 7:e605–e612
5. Bibb R, Winder J (2010) A review of the issues surrounding three-dimensional computed tomography for medical modelling using rapid prototyping techniques. *Radiography* 16:78–83
6. Santolaria J, Jiménez R, Rada M, Loscos F (2014) Error compensation method for improving the accuracy of biomodels obtained from CBCT data. *Med Eng Phys* 36:397–404
7. Winder J, Bibb R (2005) Medical rapid prototyping technologies: state of the art and current limitations for application in oral and maxillofacial surgery. *J Oral Maxillofac Surg* 63:1006–1015
8. Liang X, Lambrechts I, Sun Y, Denis K, Hassan B, Li L, Pauwels R et al (2010) A comparative evaluation of cone beam computed tomography (CBCT) and multi-slice CT (MSCT). Part II: on 3D model accuracy. *Eur J Radiol* 75:270–274
9. Salmi M, Paloheimo KS, Tuomi J, Wolff J, Mäkitie A (2013) Accuracy of medical models made by additive manufacturing (rapid manufacturing). *J Craniomaxillofac Surg* 41:603–609
10. Lermen CA, Liedke GS, Silveira HED, da Silveira HL, Mazzola AA, de Figueiredo JA (2010) Comparison between two tomographic sections in the diagnosis of external root resorption. *J Appl Oral Sci* 183:303–307
11. Ziegler CM, Woertche R, Brief J, Hassfeld S (2002) Clinical indications for digital volume tomography in oral and maxillofacial surgery. *Dentomaxillofac Radiol* 31:126–130
12. Nakagawa Y, Kobayashi K, Ishii H, Mishima A, Ishii H, Asada K et al (2002) Preoperative application of limited cone beam computerized tomography as an assessment tool before minor oral surgery. *Int J Oral Maxillofac Surg* 31:322–326
13. Liedke GS, da Silveira HE, da Silveira HL, Dutra V, de Figueiredo JA (2009) Influence of voxel size in the diagnostic ability of cone beam tomography to evaluate simulated external root resorption. *J Endod* 35:233–235
14. Berry E, Brown JM, Connell M, Craven CM, Efford ND, Radjenovic A et al (1997) Preliminary experience with medical applications of rapid prototyping by selective laser sintering. *Med Eng Phys* 19:90–96
15. Kragsskov J, Sindet-Pedersen S, Gyldensted C, Jensen KL (1996) A comparison of three-dimensional computed tomography scans and stereolithographic models for evaluation of craniofacial anomalies. *J Oral Maxillofac Surg* 54:402–411
16. Choi JY, Choi JH, Kim NK, Kim Y, Kim Y, Lee JK et al (2002) Analysis of errors in medical rapid prototyping models. *Int J Oral Maxillofac Surg* 31:23–32
17. Ludlow JB, Ivanovic M (2008) Comparative dosimetry of dental CBCT devices and 64-slice CT for oral and maxillofacial radiology. *Oral Surg Oral Med Oral Pathol Oral Radiol Endod* 106:106–114
18. Kwong JC, Palomo JM, Landers MA, Figueroa A, Hans MG (2008) Image quality produced by different cone-beam computed tomography settings. *Am J Orthod Dentofacial Orthop* 133:317–327
19. Ludlow JB, Laster WS, See M, Bailey LJ, Hershey HG (2007) Accuracy of measurements of mandibular anatomy in cone beam computed tomography images. *Oral Surg Oral Med Oral Pathol Oral Radiol Endod* 103:534–542
20. Silva DN, Gerhardt de Oliveira M, Meurer E, Meurer MI, Lopes da Silva JV, Santa-Bárbara A (2008) Dimensional error in selective laser sintering and 3D-printing of models for craniomaxillary anatomy reconstruction. *J Craniomaxillofac Surg* 36:443–449
21. Ibrahim D, Broilo TL, Heitz C, de Oliveira MG, de Oliveira HW, Nobre SM et al (2009) Dimensional error of selective laser sintering, three-dimensional printing and PolyJet models in the reproduction of mandibular anatomy. *J Craniomaxillofac Surg* 37:167–173
22. Schulzed D, Heiland M, Thurmann H, Adam G (2004) Radiation exposure during midfacial imaging using 4- and 16-slice computed tomography, cone beam computed tomography systems and conventional radiography. *Dentomaxillofac Radiol* 33:83–86
23. Laubele M, Jacobs R, Maes F, Schutyser F, Debaveye D, Bogaerts R et al (2006) Radiation dose vs. image quality for low-dose CT protocols of the head for maxillofacial surgery and oral implant planning. *Radiat Prot Dosimetry* 117:211–216
24. Spin-Neto R, Mudrak J, Matzen LH, Christensen J, Gotfredsen E, Wenzel A (2013) Cone beam CT image artefacts related to head motion simulated by a robot skull: visual characteristics and impact on image quality. *Dentomaxillofac Radiol* 42:32310645
25. Schulze R, Heil U, Gross D, Bruellmann DD, Dranischnikow E, Schwanecke U et al (2011) Artefacts in CBCT: a review. *Dentomaxillofac Radiol* 40:265–273